INTERNATIONAL JOURNAL OF AUTOMOTIVE SCIENCE AND TECHNOLOGY

2022, VOL. 6, NO: 3, 257-264 www.ijastech.org e-ISSN: 2587-0963

Optimal Clutch Control of a One-way Clutch Assistant Transmission for Electrical Vehicles

Zhi Geng[1] and Gang Li[2*]

0000-0002-4513-9984, 0000-0003-2793-4615

[1]*Shanghai Macrockets Technology Co., Ltd, Minhang, Shanghai, 201101, China*

[2]*Department of Mechanical Engineering, University of Maryland Baltimore County, Baltimore MD, 21250, United States*

Abstract

An optimal clutch control of a one-way clutch assistant transmission (OCAT) for electrical vehicles is presented in this study. The OCAT consists of a fictional clutch and a one-way clutch. The working principle of the OCAT is to shift automatically the speed ratio of the OCAT by automatic disengagement and engagement characters of the one-way clutch. Since torques in launch conditions that are generated by a motor highly oscillates, desired shift performances that can represent speed ratio changes of the OCAT also highly oscillates. A simplified dynamic model of launch conditions of the OCAT is built in this paper. The clutch controller based on an optimal control method is also proposed. Simulations and tests are carried out. The results of both simulation and test prove the dynamic model and control strategy build in the paper can be used to study the dynamic characters of the OCAT during launch.

Keywords: One-way clutch assistant transmission; Launch; Optimal clutch control; Electrical vehicles

Research Article

https://doi.org/10.30939/ijastech..1119271

Received 20.05.2022
Revised 29.06.2022
Accepted 21.07.2022

* Corresponding author
Zhi Geng
gengzhi_vali@163.com
Address: Shanghai Macrockets Technology Co., Ltd, Minhang, Shanghai, 201101, China
Tel: +86 138-1645-4123
Fax: +86 0539 5921380

1. Introduction

To improve dynamic performance and fuel efficiency of powertrain systems, some types of automatic transmissions, i.e., automatic manual transmissions (AMTs), infinitely variable transmissions (IVTs), dual clutch transmissions (DCTs), continuously variable transmissions (CVTs), and electrically variable transmissions (EVTs), are used in automotive, maritime, and renewable energy applications [1-3]. A basic function of automatic transmissions is to smoothly and efficiently convert the torque from a prime mover, e.g., a motor, to a driven part with a continuous output-to-input speed ratio. Among many different technical issues for developing these automatic transmissions, design of their control systems are crucial to achieve continuous output-to-input speed ratios and superior fuel efficiency [4,5]. Since AMTs, DCTs, and EVTs use clutch-to-clutch shifts to adjust output-to-input speed ratios, torque interruption occurs during shifts [6,7]. Generally, gears are manufactured via hobbing [8] or forming cutting [9-11] based on the theory of gearing. For some gears with special tooth profiles, e.g., concave-convex and spiral tooth profiles, their manufacturing methods and machine-tools are complex. Since meshing performances of these gears with special tooth profiles are highly sensitive to manufacturing errors [12,13], high manufacturing accuracy of gear machine-tools is required for these gears [14-16].

Contact patterns and transmission errors are two typical methods for meshing performances evaluation of gear systems [17-19]. A tooth profile modeling method was developed to improve accuracy of tooth contact analysis for gear tooth profiles [20]. Some other meshing performances, e.g., power losses, can also be evaluated based tooth contact analysis [21-23]. Since these gears have convex-concave tooth profiles, they cannot be manufactured via standard gear manufacturing methods. During a manufacture in this way, for each of the gear modules and the radius of curvature, a different blade size and gear holder is needed. However, it's clear that these gears have many advantages, if they can be produced sufficiently in the industry [24,25]. Since these gears have better load-bearing capabilities, have a balancing feature for the axial forces, quiet operation feature and their lubrication characteristics is better than herringbone gears and spur gears [26-28]. It's noteworthy that there are number of studies carried out recently in relation to these gears [29,30].

A vehicle transmission transmits the rotating power of the energy source, whether an electric motor or an internal combustion engine (ICE), through a set of gears to a differential, the unit that spins the wheels. Any vehicle, ICE or electrical vehicles (EVs), needs more torque than speed to propel the car from a dead stop, and more speed than torque once the vehicle already has forward momentum [31,32]. The transmitting power from an EV's motor to its wheels is 89% to 98% efficient, depending on the vehicle, whereas in an ICE car, the same process from engine to wheels is only 14% to 26% efficient. A clutch controller is always designed to control the clutch during launch process. Closed-loop control is used to build the clutch controller. Closed-loop methods are mainly used to control the clutch during launch: (a) optimal control method, (b) fuzzy control method, and (c) sliding-mode control method.

Qin [33] used linear quadratic optimal control method to achieve the optimum launch control of the clutch, in which the jerk is converted to one of the restrain conditions, and the minimization of sliding friction work of the clutches is set as optimal target in control. Lu [34] found compromise between the friction loss, the shock intensity, the engine torque and the engine angular acceleration to deduce the optimal engagement laws. He also used a fuzzy control theory to calculate the driver's starting intentions. Horn [35] provided an electro-hydraulic clutch control system. The controller was based on the flatness approach. Nonlinear feed forward control was employed. Experiments were conducted by this controller, provided an accurate trajectory tracking of clutch positions [36]. Song designed a sliding-mode controller to achieve robust pressure control while avoiding the chattering effect of the clutch during launch [37]. The minimum value principle is introduced to achieve an optimal clutch engagement compromised in average shock intensity and friction wear.

A gain-scheduled feedback control is widely used in automatic transmission control [38,39]. The gain-scheduled feedback control is usually developed based on look-up tables. With an increasing number of speed ratios for different driving conditions of automatic transmissions, the number of calibrated variables in the look-up tables to guarantee smooth shifts for driving conditions quickly increases and the calibration time of the open-loop control is prolonged. Since torques generated by prime movers highly oscillates, desired shift performance that can represent transmission ratio changes of automatic transmissions also highly oscillates. To reduce the calibration time and improve the control performance of the open-loop control, some speed ratio maps [40,41] and adaptive algorithms [42,43] are developed for the calibration process.

A one-way clutch is used to transmit engine torque during shifts by a novel type of transmission presented in this paper. The controller is designed based on optimal control method to control the clutch during launch. The remaining part of this paper is organized as follows: the structure layout of the OCAT is introduced in Sec. 2. A dynamic model of the OCAT is presented in Sec. 3. An optimal clutch controller of the OCAT is developed in Sec. 4. Some simulation and experimental results of the proposed optimal clutch controller are discussed in Sec. 5. Finally, some conclusions from this study are presented in Sec. 6.

2. Structure Layout of the OCAT

The OCAT is a novel type of automatic transmissions, which shifts without traction interruption. The working principle of this type of transmission is shifting automatically by the automatic disengagement and engagement characters of the one-way clutch. The idea behind this transmission concept is to fix two manual gearboxes together as a whole. One half of the OCAT, which consists of a friction clutch, mainly transmits power from the engine. The other half, which consists of a one-way clutch, is used as power assistance during shifts. Each of the two halves of the OCAT is connected to the motor separately. The structure layout of the OCAT is shown in Fig. 1.

The OCAT can be divided into two parts: an MT-type gearbox and an assistant input shaft. When the OCAT is in launch process, it seems like an AMT. Since the synchronizer of gear 1st is engaged before launch, the fiction clutch is controlled to engage by the clutch controller. Synchronizers of other gears are disengaged during launch.

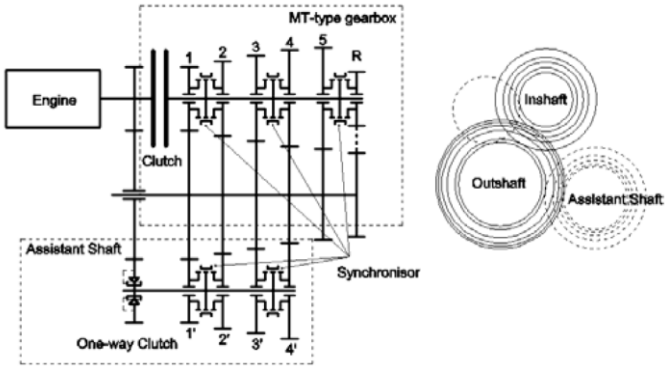

Fig. 1 Structure layout of the OCAT

3. Dynamic Model of the OCAT

A dynamic model of powertrain consisting of elements, which transmit the motor torque to wheels, is developed, as shown in Fig. 2. The synchronizer of gear 1st is ignored, since all parts of the synchronizer are connected as a static component when it is engaged. It can be seen as mass spring-damper systems for both of input shaft and output shaft. Other components of the transmission are ignored since these components have slight influences to the OCAT under the launch condition.

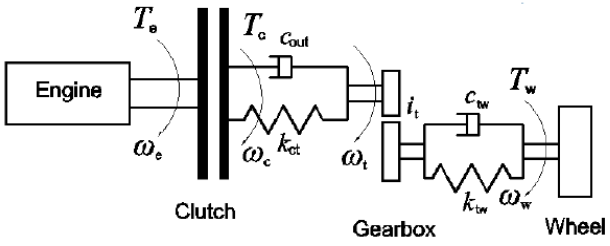

Fig. 2 Dynamic model of the powertrain in launch condition

The dynamic model of the OCAT in Fig. 2 is

$$I_e\dot{\omega}_e = T_e - T_c \tag{1}$$

where I_e is the mass moment of inertia of the rotor of the motor, ω_e is the rotational speed of the motor, T_e is the output torque of the motor, and T_c is the torque transmitted through the clutch.

$$I_c\dot{\omega}_c = T_c - k_{ct}\Delta\theta_{ct} - c_{ct}\left(\omega_c - \omega_t\right) \tag{2}$$

where I_c is the mass moment of inertia of the driven part of the clutch, ω_c is the rotational speed of the driven part of the clutch, k_{ct} is the stiffness of the input shaft, $\Delta\theta_{ct}$ is the rotational angle difference between the driven part of the clutch and the drive gear of gear 1st, c_{ct} is the damping of the input shaft, and ω_t is the rotational speed of the input shaft.

$$I_t\dot{\omega}_t = k_{ct}\Delta\theta_{ct} + c_{ct}\left(\omega_c - \omega_t\right) - \frac{1}{i_t}\left[k_{tw}\Delta\theta_{tw} + c_{tw}\left(\frac{\omega_t}{i_t} - \omega_w\right)\right] \tag{3}$$

where I_t is the equivalent mass moment of inertia of the input shaft, the output shaft, and synchronizers on the main input shaft, i_t is the speed ratio of gear 1st, k_{tw} is stiffness of the output shaft and the axle shafts of the EV, $\Delta\theta_{tw}$ is the rotational angle difference between the driven gear of gear 1st and the output shaft, c_{tw} is the damping of the output shaft and the axle shafts of the EV, and ω_w is the rotational speed of the wheel.

$$I_\omega\dot{\omega}_w = k_{tw}\Delta\theta_{tw} + c_{tw}\left(\frac{\omega_t}{i_t} - \omega_w\right) - T_w \tag{4}$$

where I_ω is the equivalent mass moment of inertia of wheels and the EV, and T_w is the output torque of wheels. The speed ratio of gear 1st, which contains the speed ratio of the gearbox i_g and the differential gear ratio i_0, can be represented as

$$i_t = i_g \cdot i_0 \tag{5}$$

The clutch is locked at the end of the engagement. Speeds of the drive and driven parts of the clutch are the same, which means the clutch rotates as a whole component. Based on Eqs. (1) and (2), one has

$$\left(I_e + I_c\right)\dot{\omega}_e = T_e - k_{ct}\Delta\theta_{ct} - c_{ct}\left(\omega_c - \omega_t\right) \tag{6}$$

When the clutch is locked, the friction disc is connected to the input shaft, which means $\omega_c = \omega_t$, Eqs. (2) and (3) can be written as

$$\left(I_c + I_t\right)\dot{\omega}_c = T_c - \frac{1}{i_t}\left[k_{tw}\Delta\theta_{tw} + c_{tw}\left(\frac{\omega_t}{i_t} - \omega_w\right)\right] \tag{7}$$

4. Clutch Controller Design

Jerk and sliding friction work are the most two important characters to measure whether the engagement of the clutch is quick enough or not. The objective function is built based on jerk and slipping energy calculated as following:

Jerk is the differential of the longitudinal acceleration of the vehicle. The acceleration is calculated by the engine torque transmitted to the wheels, which can be represented as

$$j = \frac{\mathrm{d}a}{\mathrm{d}t} = \frac{i_g i_0 \eta_T}{\delta M r_r}\frac{\mathrm{d}T_e}{\mathrm{d}t} \tag{8}$$

where a is the acceleration of the EV, M is the mass of the EV, δ is the equivalent rotational inertia of the geartrain, r_r is the equivalent radius of the wheel, and η_T is the efficiency of the gearbox.

Sliding friction work is used to evaluate the power loss, which can be represented as

$$W_c = \int_0^{t_{c1}} T_c(t)\omega_c(t)\mathrm{d}t + \int_{t_{c1}}^{t_{c2}} T_c(t)\left(\omega_e(t) - \omega_c(t)\right)\mathrm{d}t \tag{9}$$

where t_{c1} is the time when the EV begins to move, and t_{c2} is the start time of the synchronization of the motor and the clutch. The control objective function can be represented as

$$\min f = \alpha \cdot j + \beta \cdot W_c \tag{10}$$

where α and β are weighting factors of jerk and friction work, respectively. There are five working conditions with different factors group of α and β, as shown in Table 1. The lowest engagement of the clutch is controlled as Condition A, and the fastest engagement of the clutch is controlled as Condition E.

Table 1. Design parameters of the rack-pinion system

Working conditions	α	β
Condition A	1.0	0
Condition B	0.6	0.4
Condition C	0.5	0.5
Condition D	0.4	0.6
Condition E	0	1.0

5. Simulation and Experimental Results of the Clutch Controller

5.1 Simulation Results of the Clutch Controller

Simulation based on the dynamic model of the OCAT and the optimal clutch controller is conducted by using Matlab/Simulink. The motor throttle of 10% and 100% is taken into account when the EV is on the level road. The mode of the clutch is set to group A and E, which simulate the conditions of the slowest and fastest engagement of the clutch. The weighting factors of α and β are set to (1,0) and (0,1) during two conditions. The motor speed and the

speed of the output shaft are used as the input signal of the clutch controller. As the synchronizer of gear 1st is engaged during the engagement of the clutch, the speed of the output shaft is related to the speed of the driven part of the clutch.

The displacement of the fiction disc of the clutch is depicted in Fig.3. The clutch engages slowly when throttle is 10%, because jerk is 1 in this condition (Fig. 3(a)). The fiction clutch moves quickly during 1 s and 1.3 s. Then its speed comes to slow between 1.3 s and 1.9 s. The clutch engages fast again at the end of the engagement. The displacement of the clutch working in throttle of 100% is shown in Fig. 3(b), where engagement of the clutch takes less time than that in Fig. 3(a).

The clutch rotational speed is depicted, as shown in Fig. 4. Jerk in the two conditions are depicted, as shown in Fig. 5. The simulation results show the differences between two control logic while one is the fast launch and the other is slow launch.

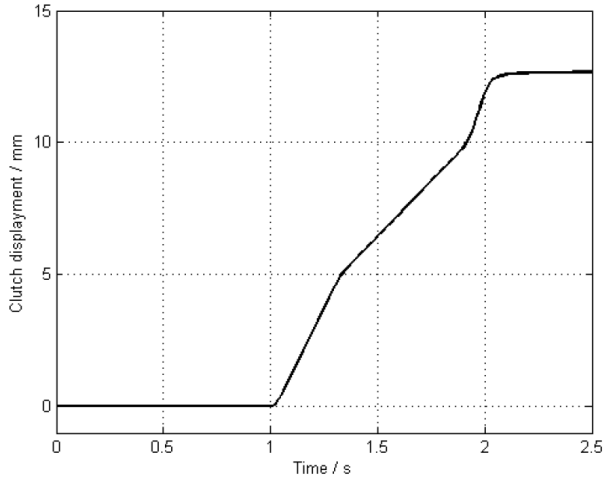

(a) Throttle of the motor is 10%

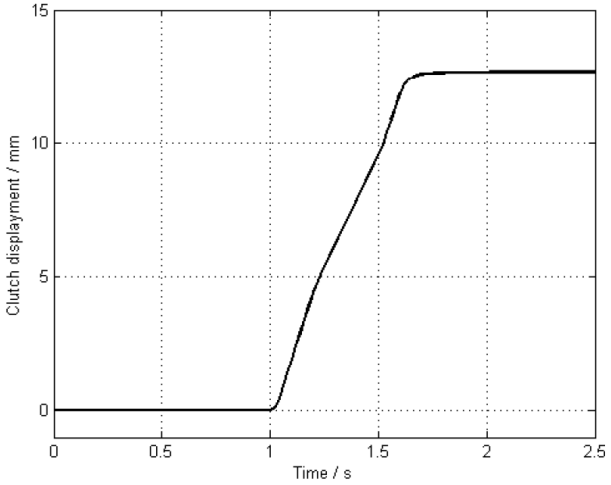

(b) Throttle of the motor is 100%

Fig. 3 Simulation results of displacement of the clutch

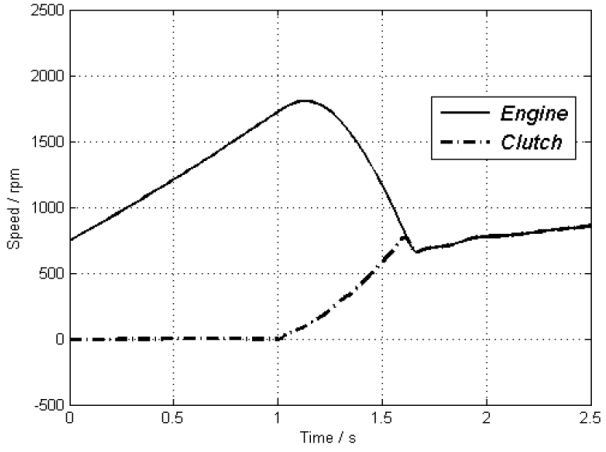

(a) Throttle of the motor is 10%

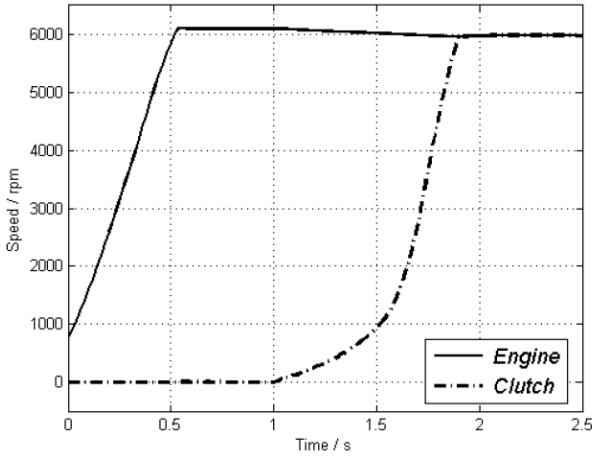

(b) Throttle of the motor is 100%

Fig. 4 Simulation results of rotational speeds of the clutch and the motor

5.2 Experimental Results of the Clutch Controller

A bench test consists of a diesel engine, a 5-speed manual gearbox, a clutch actuator, shifts actuators and a control unit is composed in this study. Load is providing by a water-power dynamometer. Sensors for the test include an engine speed sensor, an input shaft speed sensor, an output shaft speed sensor, a speed sensor of the water-power dynamometer, a position sensor of the clutch, position sensors of the gears and the accelerator pedal. The working principle of the test bench is shown in Fig. 6. Equipment and parameters of the test rig are reported in Table 2.

The clutch is forced to engage and disengage by a DC motor. The motor's current and voltage are observed during action of the clutch. The position of the driven part of the clutch is calculated by the clutch controller. The current and voltage of the motor during disengagement and engagement of the clutch is depicted in Fig.7. Fig. 7(a) shows the current raises up to 7 A as maximum during the disengagement of the clutch. At the end of disengagement, the currents raise up to 9 A due to the performance of the motor which may lead to an error. Fig. 7(b) shows that currents go to 4.2 A as maximum during the engagement of the clutch. At the end of the engagement of the clutch, the increase of currents is due to the stop

of the movement of the driven part of the clutch.

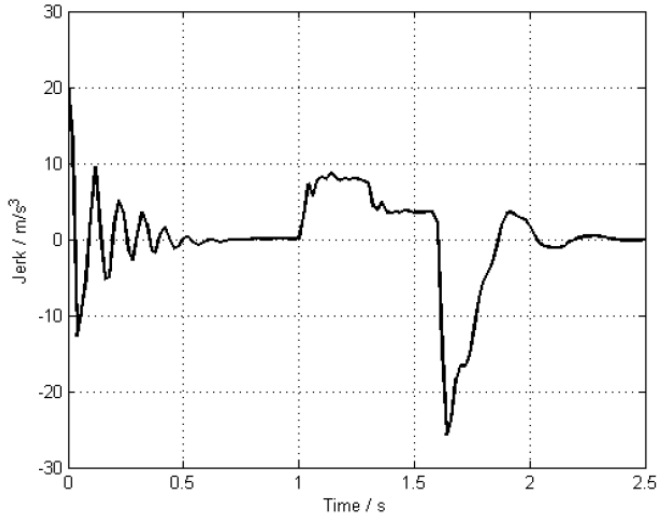

(a) Throttle of the motor is 10%

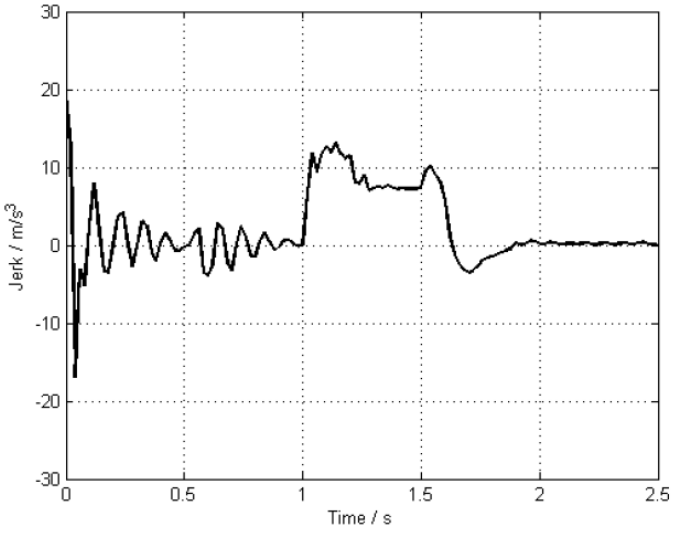

(b) Throttle of the motor is 100%

Fig. 5 Simulation results of jerk of the EV

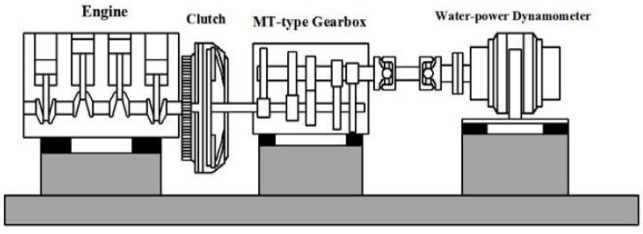

Fig. 6 Layout of the experimental setup of the OCAT testing bench

Table 2. Equipment and parameters of the experimental setup of the OCAT

Items	Type or Parameters
Load	Taian, 12PSB-HT, Water power dynamometer
Accelerator pedal	Nissan, 3000 H
Position sensor of the clutch	Rotary slide rheostat, accuracy 0.1%
Throttle sensor	Rotary slide rheostat, accuracy 0.1%
Gear position sensor	Linear slide rheostat, accuracy 0.1%
Motor speed sensor	Magneto-electrical, Voltage peak: 5.4 V
Input speed sensor of gearbox	Hall, Voltage peak: 12 V
Output speed sensor of gearbox	Hall, Voltage peak: 12 V

Table 3. System parameters of the OCAT

Items	Values
Mass moment of inertia of the driven part of the clutch I_c	2.9 kg m^2
Equivalent mass moment of inertia of the input shaft, the output shaft, and synchronizers on the main input shaft I_t	36 kg
Damping of the input shaft c_{ct}	0.21
Stiffness of the input shaft k_{ct}	2,600 N/m

Sensors of engine speeds, speeds of the input shaft of the gearbox, and positions of the driven part of the clutch are indicated as dynamic characters of the powertrain. Rotational speeds and displacement of the driven part of the gearbox are depicted in Fig. 8. The control algorithm profiles of the test are based on the simulations presented in the Section 4. The differences between the simulations and tests are the throttle of the engine, because of the engine speed is too high in the condition of full-throttle. Weighting factors of α and β are defined to (1, 0) as the throttle is 5%, and to (0.6, 0.4) as the throttle is 10% in the test.

The speed of the input shaft of the gearbox synchronizes the engine speed at 0.26 s when the throttle is 5% (Fig.8 (a)), while the time of synchronization is 0.15 s when the throttle is 10% (Fig.8 (c)). The clutch is forced to engage following the rule of 'fast-slow-fast' in the both two conditions (Fig. 8(b) and (d)), which is similar to the control algorithm profile of the clutch on AMT. Speed fluctuations of the output speed of the OCAT are caused by the impulse rate and oscillations of the OCAT, as shown in Fig. 8. The impulse rate and oscillations of the OCAT can be decreased with reduction the calibration time and improvement the control performance of the clutch control.

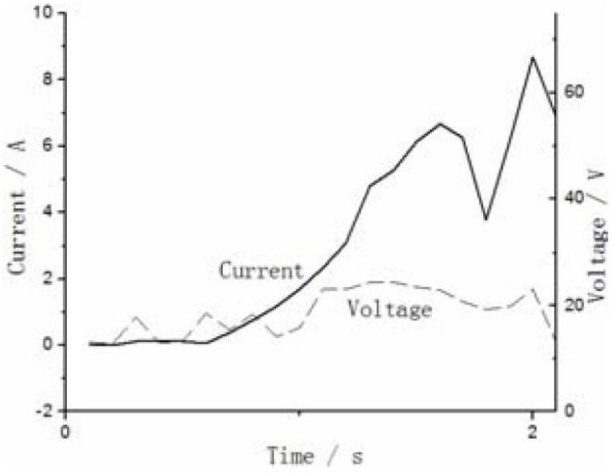

(a) Disengagement

(b)

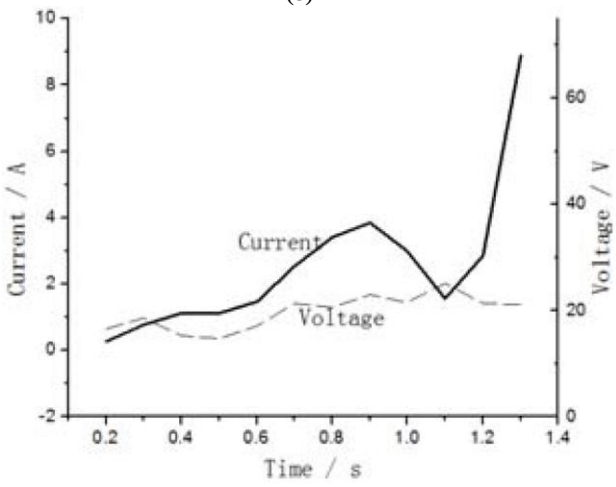

(b) Engagement

Fig. 7 Current and voltage of the motor during action of the clutch

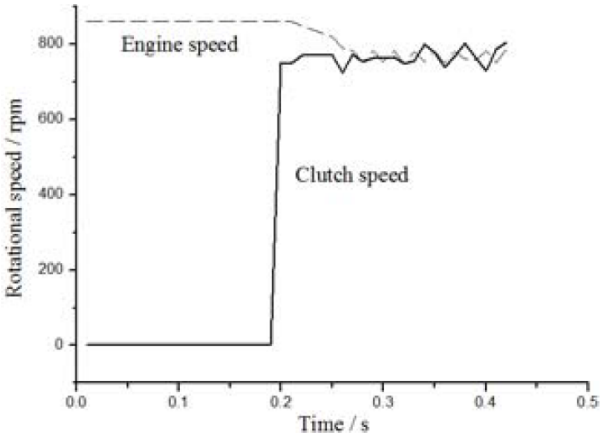

(a) Rotational speed at throttle of 5%

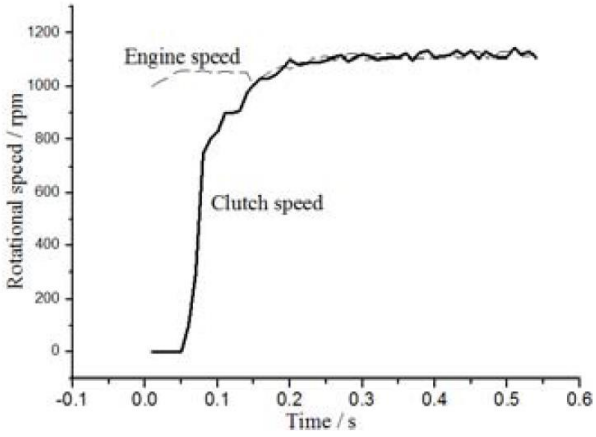

(c) Rotational speed at throttle of 10%

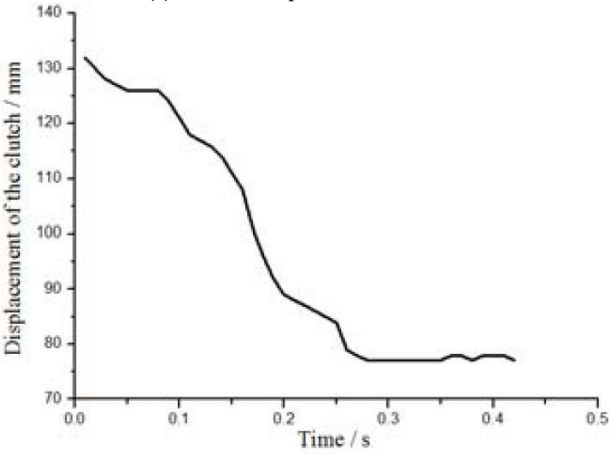

(b) Displacement at throttle of 5%

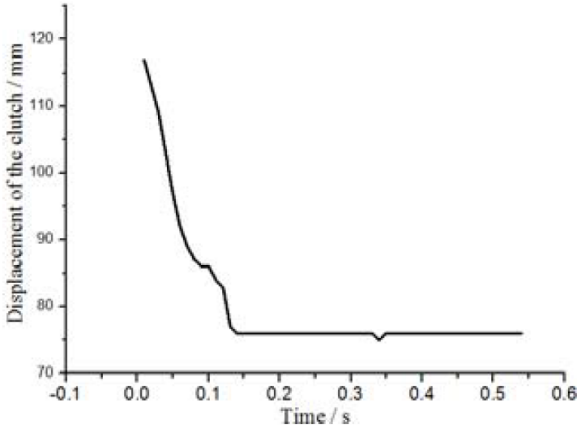

(d) Displacement at throttle of 10%

Fig. 8 Test results of the dynamic characters during launch

6. Conclusions

As a novel type of automatic transmission, the OCAT has the similar dynamic characters with that on AMT during launch. The dynamic model presented in this paper is appropriate to simulate the process of launch. A new optimal control strategy for the OCAT is developed for high-performance clutch control of the OCAT system. The primary merit of the proposed optimal controller for the OCAT lies in the fact that an accurate and complete model-based approach can establish a tracking error model for desired control values in varying operating conditions with arbitrary input speeds.

The proposed control strategy with the tracking error model exhibits good control performance of the speed ratio of the OCAT system with a variable input speed. The proposed optimal controller for the OCAT could control the engagement and disengagement of the clutch in launch conditions under different throttle angles. Experimental results show that the control strategy can adjust and stabilize the speed ratio of the OCAT system for the desired output speed. The control strategy of the OCAT system can achieve fluctuations of the output speed and the speed ratio within 2% and 3% for constant and variable input speeds, respectively. The proposed control strategy can be used to promote commercialization of the OCAT for EV applications.

Acknowledgment

The author is grateful for the financial support from the Shanghai Education Commission, Science and Technology Innovation Projects, Grant No. 11CXY45.

Conflict of Interest Statement

There is no conflict of interest in the study.

CRediT Author Statement

Zhi Geng: Conceptualization, Writing-original draft, Data curation, Software.
Gang Li: Conceptualization, Supervision, Writing-review&editing, Validation,

Nomenclature

I_e : Mass moment of inertia of the rotor of the motor
I_c : Mass moment of inertia of the driven part of the clutch
I_t : Equivalent mass moment of inertia of the input shaft, the output shaft, and synchronizers on the main input shaft
I_ω : Equivalent mass moment of inertia of wheels and the EV
ω_e : Rotational speed of the motor
ω_c : Rotational speed of the driven part of the clutch
T_e : Output torque of the motor
T_c : Torque transmitted through the clutch
T_w : Output torque of wheels
c_{ct} : Damping of the input shaft
c_{tw} : Damping of the output shaft and the axle shafts of the EV
k_{tw} : Stiffness of the output shaft and the axle shafts of the EV
k_{ct} : Stiffness of the input shaft
i_t : Speed ratio of gear 1st
i_0 : Differential gear ratio
i_g : Speed ratio of the gearbox
$\Delta\theta_{ct}$: Rotational angle difference between the driven part of the clutch and the drive gear of gear 1st
$\Delta\theta_{tw}$: Rotational angle difference between the driven gear of gear 1st and the output shaft

References

[1] Srivastava N, Haque I. A review on belt and chain continuously variable transmissions (CVT): Dynamics and control. Mech Mach Theory. 2009;44(1):19-41.
[2] Hu YH, Li G, Zhu WD, Cui JK. An elastic transmission error compensation method for rotary vector speed reducers based on error sensitivity analysis. Appl Sci. 2020;10(2):481.
[3] Yan J, Li G, Liu K. Development trend of wind power technology. Int J Adv Eng Res Sci. 2020;7(6):124-132.
[4] Zhu Y, Liu KC. The present situation of research and development of impulse stepless speed variator. Pack Food Mach. 2003;21(5):11-14.
[5] Li G. Design and modeling of an impulse continuously variable transmission with a rotational swashplate. Int J Auto Sci Tech. 2020;4(4):307-313.
[6] Xu M, Zhang X, Hu G, Li G. The structure design and flow field simulation of a fire water monitor driven by worm gear with bevel gear. Mach Tool & Hydra. 2016;6:57-61.
[7] Gu KL, Wang ZH, Li G, Liu XR. Optimization of geometric parameters of the straight conjugate internal gear pump based on GA. Elec Sci Tech, 2017;30(6):39-42.
[8] Zhang XL, Wang ZH, Li G. Research on virtual hobbing simulation and study of tooth surface accuracy of involute helical gears. Appl Mech Mater. 2012;155:601-605.
[9] Li G, Wang ZH, Zhu WD, Kubo A. A function-oriented active form-grinding method for cylindrical gears based on error sensitivity. Int J Adv Manuf Tech. 2017;92(5-8):3019-3031.
[10] Wang ZH, Zhu WM, Li G, Geng Z. Optimization of contact line for form-grinding modified helical gears based on neural network. China Mech Eng. 2014;25(12):1665-1671.
[11] Li G. An active forming grinding method for cylindrical involute gears based on a second-order transmission error model. SCIREA J Mech Eng. 2019;2(1):1-14.
[12] Li G, Zhu WD. An active ease-off topography modification approach for hypoid pinions based on a modified error sensitivity analysis method. ASME J Mech Des. 2019;141(9):093302.
[13] Li G, Wang ZH, Kubo A. Error-sensitivity analysis for hypoid gears using a real tooth surface contact model. Proc Instn Mech Eng, Part

C: J Mech Eng Sci. 2017;231(3):507-521.

[14]Zhang WX, Wang ZH, Liu XR, Li G, Wan PL, Wang W. Research on optimization of temperature measuring point and thermal error prediction method of CNC machine tools. J Shaanxi University of

[16]Wang ZH, Song XM, He WM, Li G, Zhu WM, Geng Z. Tooth surface model construction and error evaluation for tooth-trace modification of helical gear by form grinding. China Mech Eng. 2015;26(21):2841-2847.

[17]Li G, Wang ZH, Kubo A. Tooth contact analysis of spiral bevel gears based on digital real tooth surfaces. Chin J Mech Eng. 2014;50(15):1-11.

[18]Wang ZH, Wang J, Ma PC, Li G. Dynamic transmission error analysis of spiral bevel gears with actual tooth surfaces. J Vib Shock. 2014;33(15):138-143.

[19]Wang ZH, Wang J, Wang QL, Li G. Transmission error of spiral bevel gear based on finite element method. J of Vib Shock. 2014;33(14):165-170.

[20]Li G, Wang ZH, Kubo A. The modeling approach of digital real tooth surfaces of hypoid gears based on non-geometric-feature segmentation and interpolation algorithm. Int J Prec Eng Manuf. 2016;17(3):281-292.

[21]Li G, Zhu WD. Design and power loss evaluation of a noncircular gear pair for an infinitely variable transmission. Mech Mach Theory. 2021;156:104137.

[22]van Berkel K, Hofman T, Vroemen B, Steinbuch M. Optimal control of a mechanical hybrid powertrain. IEEE Trans Vehic Tech. 2012;61(2):485-497.

[23]Li G, Geng Z. Gear bending stress analysis of automatic transmissions with different fillet curves. Int J Auto Sci Tech. 2021;5(2):99-105.

[24]Huang DQ, Wang ZH, Li G, Zhu WD. Conjugate approach for hypoid gears frictional loss comparison between different roughness patterns under mixed elastohydrodynamic lubrication regime. Tribo Int. 2019;140:105884.

[25]Li G, Wang ZH, Zhu WD. Prediction of surface wear of involute gears based on a modified fractal method. ASME J Tribo. 2019;141(3):031603.

[26]Wu J, Wang ZH, Li G. Study on crack propagation characteristics and remaining life of helical gear. J Mech Trans. 2014;38(12):1-4.

[27]Li G, Wang ZH, Geng Z, Zhu WM. Modeling approach of digital real tooth surfaces of hypoid gears based on non-geometric-feature segmentation and interpolation algorithm. Chin J Mech Eng. 2015;51(7):77-84.

[28]Li G, Geng Z. Tooth contact analysis of herringbone rack gears of an impulse continuously variable transmission. Int J Auto Sci Tech. 2021;5(1):52-57.

[29]Wang ZH, Yuan KK, Li G. Optimization identification for dynamic

Tech (Na Sci Ed). 2017; 33(3):18-24.

[15]Wang ZH, Cao H, Li G, Liu XR. Compensation of the radial error of measuring head based on forming grinding machine. J Mech Trans. 2017;41(3):143-146.

characteristics parameters of sliding joints based on response surface methodology. China Mech Eng. 2016;27(5):622-626.

[30]Hu YH, Li G, Hu AM. Iterative optimization of orbital dynamics based on model prediction. Front Arti Intel App. 2019;320:76-86.

[31]Li G, Zhu WD. Experimental investigation on control of an infinitely variable transmission system for tidal current energy converters. IEEE/ASME Trans Mechatron. 2021; 26(4):1960-1967.

[32]Li G, Zhu WD. Theoretical and experimental investigation on an integral time-delay feedback control combined with a closed-loop control for an infinitely variable transmission system. Mech Mach Theory. 2021;164:104410.

[33]Qin DT. Universal clutch starting control of AMT/DCT automatic transmission based on optimal control. Chin J Mech Eng. 2011;47(12):85-91.

[34]Lu TL, Dai F, Zhang JW, Wu MX. Optimal control of dry clutch engagement based on the driver's starting intentions. Proc Instn Mech Eng, Part D: J Automob Eng. 2012; 226(8):1048-1057.

[35]Horn J, Bamberger J, Michau P, Pindl S. Flatness-based clutch control for automated manual transmissions. Control Eng Pract. 2003;11:1353-1359.

[36]Li G, Zhu WD. Time-delay closed-loop control of an infinitely variable transmission system for tidal current energy converters. Renew Energy. 2022;189:1120-1132.

[37]Song XY, Sun ZX. Pressure-based clutch control for automotive transmissions using a sliding-mode controller. IEEE/ASME Trans Mechatron. 2012;17(3):534-546.

[38]Kulkarni M, Shim T, Zhang Y. Shift dynamics and control of dual-clutch transmissions. Mech Mach Theory. 2007;42(2): 168–182 .

[39]Srivastava N, Haque I. A review on belt and chain continuously variable transmissions (CVT): dynamics and control. Mech Mach Theory. 2009;44(1): 19–41.

[40]Bertini L, Carmignani L, Frendo F. Analytical model for the power losses in rubber V-belt continuously variable transmission (CVT). Mech Mach Theory. 2014;78: 289–306 .

[41]Ryu W, Kim H. CVT Ratio control with consideration of CVT system loss. Int J Automot Technol. 2008;9(4): 459–465.

[42]Shi G, Dong P, Sun H, Liu Y, Cheng Y, Xu X, Adaptive control of the shifting process in automatic transmissions. Int J Automot Technol. 2017;18(1): 179–194.

[43]Elzaghir W, Zhang Y, Natarajan N, Massey F, Mi CC. Model reference adaptive control for hybrid electric vehicle with dual clutch transmission configurations, IEEE Trans Veh Technol. 2018;67(2): 991–999.